

A novel Mo-W interlayer approach for CVD diamond deposition on steel

Vojtěch Kundrát,¹ Xiaoling Zhang,² Kevin Cooke,² Hailin Sun,² John Sullivan,¹ and Haitao Ye^{1,a}

¹*School of Engineering & Applied Science, Aston University, Birmingham, B4 7ET, United Kingdom*

²*Miba Coating Group: Teer Coatings Ltd, West-Stone-House, West-Stone, Berry-Hill-Industrial-Estate, WR9 9AS, Droitwich, United Kingdom*

(Received 9 December 2014; accepted 10 April 2015; published online 20 April 2015)

Steel is the most widely used material in engineering for its cost/performance ratio and coatings are routinely applied on its surface to further improve its properties. Diamond coated steel parts are an option for many demanding industrial applications through prolonging the lifetime of steel parts, enhancement of tool performance as well as the reduction of wear rates. Direct deposition of diamond on steel using conventional chemical vapour deposition (CVD) processes is known to give poor results due to the preferential formation of amorphous carbon on iron, nickel and other elements as well as stresses induced from the significant difference in the thermal expansion coefficients of those materials. This article reports a novel approach of deposition of nanocrystalline diamond coatings on high-speed steel (M42) substrates using a multi-structured molybdenum (Mo) – tungsten (W) interlayer to form steel/Mo/Mo-W/W/diamond sandwich structures which overcome the adhesion problem related to direct magnetron sputtering deposition of pure tungsten. Surface, interface and tribology properties were evaluated to understand the role of such an interlayer structure. The multi-structured Mo-W interlayer has been proven to improve the adhesion between diamond films and steel substrates by acting as an effective diffusion barrier during the CVD diamond deposition. © 2015 Author(s). All article content, except where otherwise noted, is licensed under a Creative Commons Attribution 3.0 Unported License. [<http://dx.doi.org/10.1063/1.4918969>]

I. INTRODUCTION

Diamond thin films are of great interest for industrial use due to their outstanding tribological properties such as high hardness, low wear and tear rates, low friction coefficient and chemical resistance.¹ Chemical vapour deposition (CVD) is a well-established method to grow diamond films on a range of substrate materials. Steel is the widely-used industry material for tool manufacture and mechanical assemblies due to its mechanical characteristics, price and divisibility of all its possible compositions tailored for specific uses. Surface enhancement of steel parts can be done through application of a wide range of coatings which provide the surface with corrosion prevention, wear enhancement, esthetical factors, etc. Therefore, the steel substrates with deposited CVD diamond coatings have become the primary focus of this research. For a good quality and well performing diamond films on ferrous substrates it is essential to obtain excellent adhesion between steel and the diamond while at the same time maintaining the intrinsic properties of the steel.

However, direct deposition of nanocrystalline diamond onto steel substrates gives poor results in terms of diamond film growth, its adhesion with steel surface as well as for cross-diffusion of elements between steel substrate and as-grown diamond film.^{2,3} Chemical elements, such as iron (Fe) and cobalt (Co), greatly affect diamond formation in terms of facilitating the formation of

^aCorresponding author: h.ye@aston.ac.uk



amorphous carbon layer before any diamond growth is feasible, deteriorating adhesion between steel and diamond. At the same time diffusion of carbon into the steel carburizes steel surface and changes steel properties. In order to tackle the adhesion problem different types of interlayers have been used on ferrous substrates such as chromium (Cr), titanium (Ti), Mo, W, nitrides, carbides and multi-structured interlayers,^{2,4-11} among which, W interlayers as well as Mo interlayers have demonstrated exceptionally promising properties. However, most of the research on tungsten interlayer was reported on silicon substrates¹²⁻¹⁴ and little on metallic substrates.¹⁵ W is a very effective diffusion barrier against Fe⁸ and C⁷ and a strong carbide forming material.⁸ Such properties are much desired for depositing good quality diamond films. Mo is a great bonding material, which adheres strongly to steel as well as to tungsten. Moreover both W and Mo can serve as a thermal stress buffer layer as their thermal expansion coefficients (W: $4.7 \times 10^{-6} \text{ K}^{-1}$ and Mo: $5.8 \times 10^{-6} \text{ K}^{-1}$) lay between M42 steel ($12.5 \times 10^{-6} \text{ K}^{-1}$) and diamond ($2.8 \times 10^{-6} \text{ K}^{-1}$) at the temperature range of 20-800 °C.^{16,17}

In order to overcome the adhesion problem associated with W-only interlayers, novel multi-structured Mo-W interlayers have been employed here. The advantage and novelty of the proposed Mo-W interlayers lie in the following aspects: (a) they can avoid the formation of the Fe-W intermetallics; (b) they offer tailored gradient deposition due to the complete miscibility¹⁸ between Mo and W; (c) no similar multi-structured interlayers have been used to facilitate the diamond growth on steel substrates. This paper reports the studies of the combination of Mo-W coatings as an interlayer for diamond films growth on steel substrates.

II. EXPERIMENTAL DETAILS

High-speed steel (M42) discs (diameter: 25 mm; thickness: 3 mm) were polished to a mirror finish using abrasive papers up to 1200 grid as the base substrates. Teer Coatings limited (TCL) industrial close-field-unbalanced-magnetron-sputtering (UDP 650) coating system equipped with four magnetrons arranged at 90° was used for deposition of W and Mo-W films.¹⁹ Two opposing magnetrons were alternatively used for sputtering W and Mo, respectively. During the sputtering process, samples mounted on substrate holders were rotated at the fixed speed (4 rpm) to ensure the uniformity of the sputtered coatings.

Deposition of Mo-W interlayers was performed in three steps. Firstly a thin layer of Mo (100-200 nm) was sputtered; followed co-sputtering of the transition layer of Mo-W (100-200 nm) and finally a layer of W (≈ 800 nm) was deposited. Total thickness of sputtered Mo-W multi-structured interlayer was 1.1 μm . A tungsten-only interlayer of the same thickness was also sputtered on to M42 steel substrates. As-sputtered samples were cleaned by ultrasonication in acetone, isopropanol and deionised water.

Seki ASTeX AX5010 microwave plasma CVD deposition system (MPCVD) was used for diamond deposition. Nanodiamond (ND) suspension (0.2 wt. % of ND of less than 10 nm size in deionised water; agitated for 30 min) was prepared firstly; steel samples were subsequently immersed in it for 30 s. In order to remove the excess of diamond particles from the sample surface, samples were flushed with deionised water and blow dried in a nitrogen flow. Deposition conditions were: microwave power 550 W; pressure 25 Torr; 3 vol. % of CH₄ in H₂; total gas flow 200 sccm; sample surface temperature 785 °C; time 2 h. Deposition chamber was evacuated after the deposition and samples were cooled down by radiation cooling to minimize the effect of thermal shock. Sample's surface temperature was measured using thermocouple on the backside of the substrate holder and verified by the Infrared temperature sensor.

Thickness and adhesion of deposited Mo-W and pure W coatings were tested using ball crater method (BC-2 Ball Crater Device) and Rockwell C indentation. Surface and near-surface characterization techniques employed in this study were X-ray diffraction (XRD, Siemens D5000 diffractometer at 2° glancing angle), scanning electron microscopy (SEM), energy-dispersive X-ray spectroscopy (EDX), atomic force microscopy (AFM, Autoprobe M5). Thickness of diamond films was measured using profilometer (Talystep, Taylor-Hobson). Adhesion was evaluated through Teer's ST3001 scratch tester equipped with WC ball (5 mm) on scratches of 5-30 N at 100 N/min loading

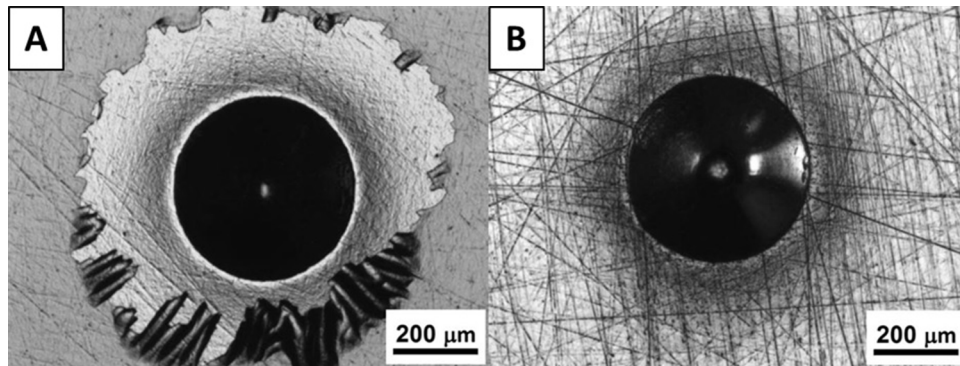


FIG. 1. (a) Rockwell C indent into W coated steel; (b) Rockwell C indent into Mo-W coated steel.

rates and velocity of 10 mm/min. Critical load was then derived from the distance to the first sign of chipped diamond coatings from the racetrack.

III. RESULTS AND DISCUSSION

Good adhesion between the proposed interlayers and steel substrates is critical for subsequent growth of high quality diamond films. Fig. 1 compares the results from Rockwell C indentations performed on W-only interlays and multi-structured Mo-W interlayers. Direct sputtering of tungsten onto steel resulted in poor adhesion as shown in Fig. 1(a). It can be seen that large amount of W spallation occurred around the Rockwell C indent, which is due to the formation of Fe-W intermetallics at the interface of steel-W.²⁰ Such intermetallics are tough and brittle which facilitate the detachment of W coatings from the steel substrates. Fig. 1(b) shows the Rockwell C indentation results from the multi-structured Mo-W interlayer. It reveals that no chipping or spalling around the indent is observed which implies the Mo-W interlayers have good adhesion onto steel substrates. The improved adhesion mechanism of the multi-structured Mo-W interlayers lies in: (a) Mo being a known bonding layer between steel and other deposited coatings;²¹ (b) Mo and W having total miscibility as shown in their binary diagram;¹⁸ (c) gradient transition between Mo and W across the depth of the 150-200 nm thick interlayers. Due to the adhesion failure of directly tungsten deposition onto steel as shown in Fig. 1(a), the following study will focus on Mo-W interlayers and subsequent diamond growth.

Further analysis on the surface morphology and phase composition of the Mo-W interlayers is shown in Fig. 2. Fig. 2(a) shows the SEM image of the surface of the Mo-W interlayer, which

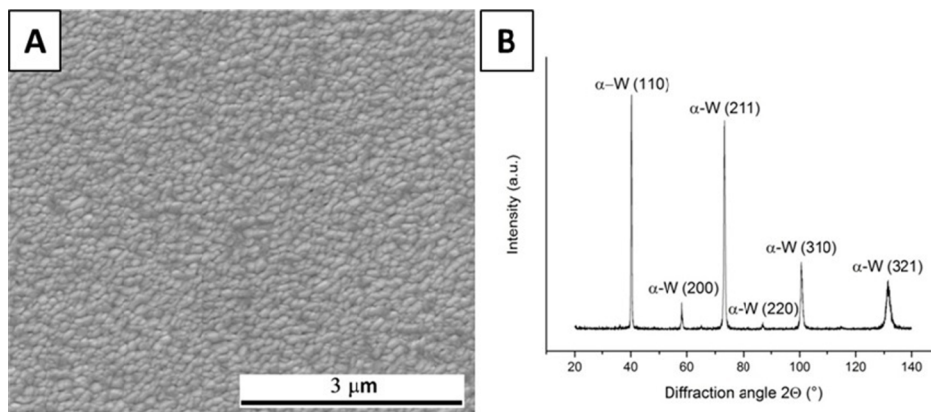


FIG. 2. Mo-W interlayer's top surface: (a) SEM image; (b) XRD spectra.

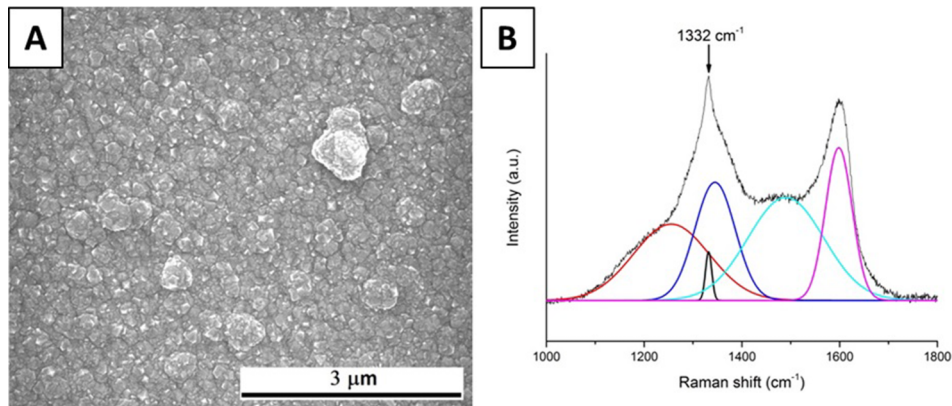


FIG. 3. Diamond film structure; (a) SEM image from Diamond surface; (b) Deconvoluted Raman spectra of diamond film.

consists of W cluster of with average grain size of 110 nm. Fig. 2(b) shows the XRD spectra of surface of the Mo-W interlayer. It can be seen that there are six differing peaks located at 40° , 58° , 73° , 87° , 101° , and 131° , which correspond to tungsten (110), (200), (211), (220), (310), and (321) crystal orientation, respectively.²² It is clear that there are no Mo, Fe or other elements present in XRD spectrum, which indicates that high purity of W was deposited during the sputtering process.

The deposition of diamond on a foreign substrate usually requires an extra nucleation stage, since diamond does not grow spontaneously on non-diamond materials. Seeding the substrate with nanodiamond particles prior to the CVD diamond growth stage provides high diamond nucleation densities and is therefore widely used. It has been recognised that sample agitation as well as mere immersion of sample into diamond colloids produces excellent coverage of samples with diamond nanoparticles.^{23–26} Here we adopted this approach by immersing samples into nanodiamond suspension. The subsequent growth of nanodiamond films was carried out using MPCVD system.

Fig. 3(a) shows the SEM image of the grown nanodiamond film on steel substrates with Mo-W interlayer with diamond grains size of 140 nm in average. The nanodiamond film has an average thickness of 260 – 300 nm (from AFM and profilometer) with roughness of 72 nm rms over 900 μm^2 area. Fig. 3(b) shows the deconvoluted Raman spectra of nanodiamond coating. There is a diamond characteristic peak located at 1332 cm^{-1} . Alongside of the diamond peak, there are other Raman peaks located at 1345 cm^{-1} and 1598 cm^{-1} , which correspond to D-peak and G-peak of sp^2 bonded carbon species.²⁷ Other Raman peaks located at 1255 cm^{-1} and 1490 cm^{-1} are also observed which are attributed to transpolyacetylene.^{27,28} The transpolyacetylene is believed to originate at the diamond grain boundaries during the CVD deposition in hydrogen rich environment.²⁸

The adhesion measurement of diamond films was performed using a scratch test. The tested sample was cleaned of any delaminated debris after the scratch test to fully expose the region of delamination. In order to ensure the reliability of the experimental data, a total of five scratch tests were repeated on diamond coated samples. The arithmetic mean value of the first sign of chipping was measured at 11.4 N. The minimal and maximal values of adhesion failure are 8.5 N and 17.4 N, respectively. During the scratch tests the material of WC ball was smeared over the diamond surface adhering to the diamond film. At the point of reaching the critical load diamond coating bulged on the surface to form the scratch trace as shown in Fig. 4. Adhesive failure occurred therefore after the release of compressive stresses when WC ball progressed further in the scratch track. The diameter of used WC ball is large enough to be inducing mostly compressive stresses rather than bending stresses on the diamond film and therefore is suitable for adhesion evaluation.²⁹ Adhesion failure of diamond film is confined to only the inside of the scratch trace with well adhering diamond film surrounding it. Lu *et al.* reported that critical load of diamond films on WC increases from 11.2 N for diamond films thickness of 1.5 μm to 14.5 N for samples with thickness of 4.5 μm .³⁰ Enderl *et al.*³¹ reported the critical load of diamond coatings on steel substrates was within the region of 6–22 N for diamond films with thickness of 3–5 μm . Whilst our diamond samples (300nm thickness) using Mo-W interlayers are much thinner than others reported, they show a similar level of critical

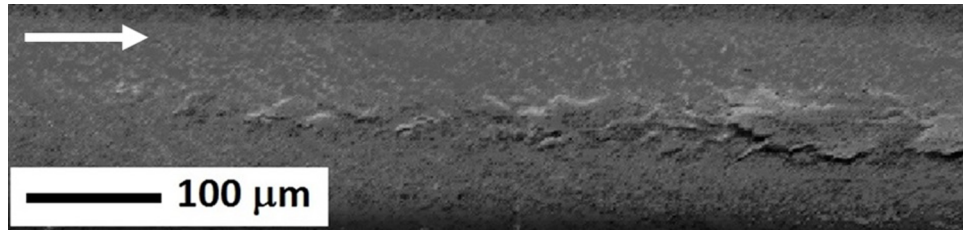


FIG. 4. SEM image of the start of delamination of diamond film within the scratch track using back scattered electrons imaging mode; white arrow shows the direction of sliding of WC ball.

loads of 11.4 N in average. It is difficult to make quantitative comparison among samples measured at different evaluation conditions from different research groups.³² This is because the surface and interface of samples is of as high importance as a precise description of testing conditions.³³ Qualitative comparison of our films with reported values can confirm similar level of adhesion properties to reflect the positive contribution of the Mo-W interlayer.

After the scratch test, SEM analysis was used to examine the surface morphology of the delaminated areas as shown in Fig. 5. Areas A and B within Fig. 5 represent the sample's surface with and without diamond films delamination, respectively. The surface morphology in area A shows the W or W_xC coatings after diamond delamination, which are similar to the SEM image in Fig. 2(a). The EDX analysis from areas A and B is summarised in Table I, together with a data obtained from unscratched part of diamond film for comparison reasons. Elements present in area A are W and C only, presumably forming W_xC , which results in the delamination at the interface between W_xC and diamond films. Elements detected in area B are O and Co in addition to W and C. The presence of tiny amount of Co and oxygen is believed to originate from the WC ball of the scratch tester. Co was used as a binder within the WC ball of the scratch tester and was likely transferred

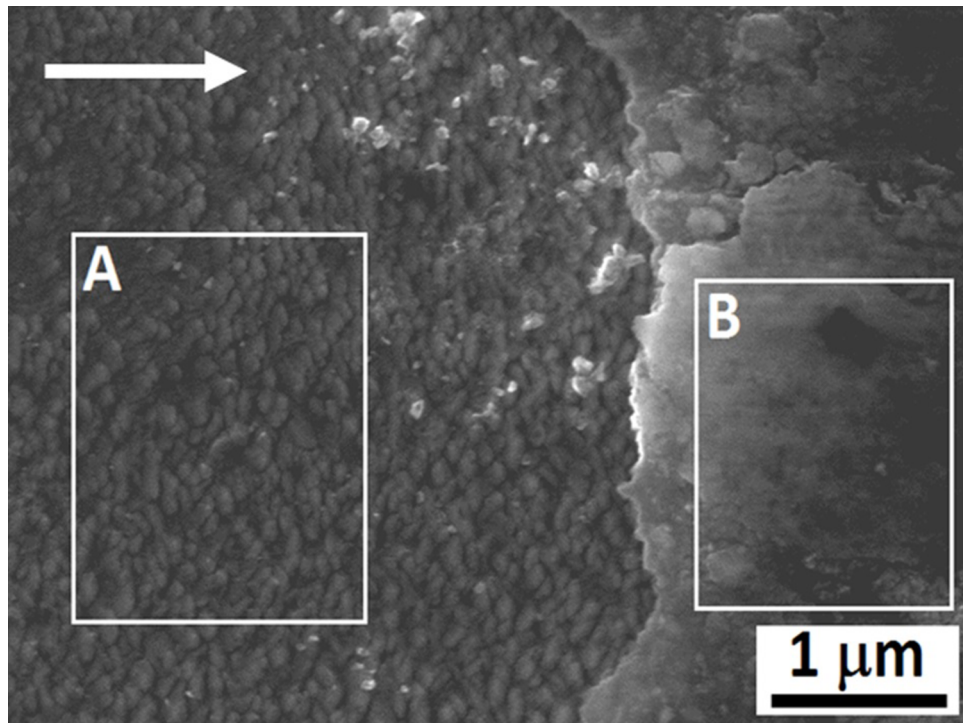


FIG. 5. SEM image of part of the scratch track; left – delaminated area; right – adherent area; rectangles A and B mark the areas of EDX scan; white arrow shows the direction of sliding of WC ball.

TABLE I. EDX spectra of delaminated, adherent parts of diamond film within scratch region and of an unscratched part of diamond film.

Elements in wt. %	EDX Spectrum of part of the scratch track					
	C	W	O	Co	Mo	Fe
A - delaminated	3.66	96.34	-	-	-	-
B - adherent	26.48	68.29	3.73	1.5	-	-
Unscratched region	45.79	54.21	-	-	-	-

onto the diamond surface during the scratch process. The amount of C present in the unscratched region is higher than that in the adherent part of the scratch track, which is due to the transfer of material from WC ball onto the diamond film as well. Comparing the EDX results from all the discussed three areas, it can be seen that there were no Mo, Fe or other steel elements detected in the whole scanned regions. This supports the effectiveness of the Mo-W interlayer as a diffusion barrier against diffusion of steel elements into the diamond film.

In order to further understand the functionality of Mo-W interlayers EDX analysis was performed across the sample's cross-section as shown in Fig. 6. Carbon intensity is naturally the highest in the region of diamond films and decreases rapidly upon encountering the W-rich side of the Mo-W interlayer. Very similar results can be seen for iron where its intensity drops at the start of Mo/steel interface. Co is also present in M42 steel (typically around 8 wt. %) and its EDX profile follows the same trend as iron. For clarity of data presentation Co distribution was not added into Fig. 6. The EDX depth profile agrees with measured thickness of diamond films (profilometer, AFM) and the thickness of Mo-W coating (ball crate). It is worth mentioning that the EDX spectra obtained doesn't possess as high spatial resolution as would be desirable.³⁴ It is reasonable to assume that the distribution contour plots between the elements are even sharper than the obtained profile in Fig. 6.

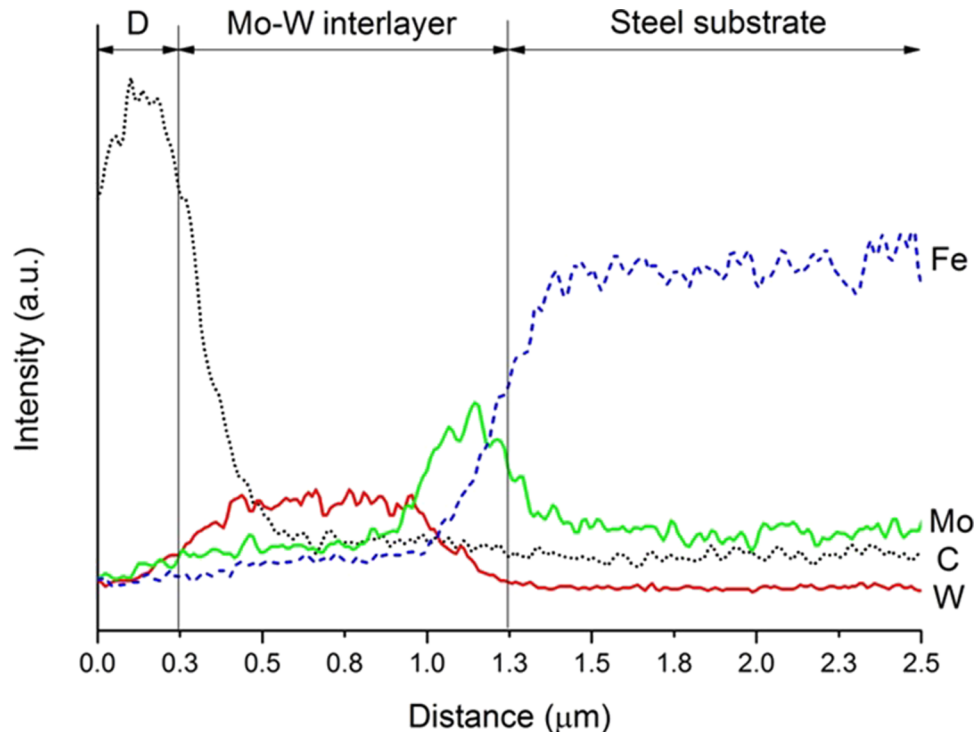


FIG. 6. EDX analysis of Diamond/Mo-W/M42 sample cross-section.

The effectiveness of Mo-W interlayer as a diffusion barrier can also be indirectly assessed through changes in sample's hardness. Long-time exposure to elevated temperature during CVD diamond growth will lead to the hardening of the steel substrates due to atomic hydrogen diffusion, carbide formation.⁴ However, the Mo-W coated steel sample before and after diamond deposition shows a slight decrease in their respective hardness from 64 HRC to 61 HRC. The unexpected softening of the samples implies the effectiveness of Mo-W interlayers being a fully functional diffusion barrier preventing diffusion of plasma species such as atomic hydrogen and carbon into the steel even after a long time high temperature CVD process.

IV. CONCLUSIONS

Nanodiamond films have been successfully grown on steel substrates with multi-structured Mo-W interlayers using PECVD method in 3% CH₄/H₂ gas mixture. The multi-structured Mo-W interlayer on steel substrates has advantages over the directly sputtering of W on steel substrates in terms of improved adhesion. Scratch tests of diamond film grown on the Mo-W interlayered substrate displayed first sign of adhesion failure at an average value of 11.4 N, which is comparable with results reported by others. Chipping of diamond films was believed to originate from the diamond/carburised tungsten interface without visible cracks shown on the sputtered Mo-W interlayer. Elemental distribution from the cross-sectional EDX scan confirms the diffusion barrier capability of Mo-W layer. Indirect Rockwell C hardness measurements shows that the Mo-W interlayer can prevent the interaction between steel and plasma radicals to avoid the brittleness of the substrates. The studied Mo-W interlayer approach offers a new possible way for further exploration of diamond coated steel parts for the tribological application.

ACKNOWLEDGMENT

This work was supported by EPSRC Nanotechnology KTN Case Studentship 'Nanodiamond Coatings for Advanced Engineering Application', in collaboration with Miba Coating Group, Austria and Teer Coatings Ltd, UK.

- ¹ P.W. May, *Philos. Trans. R. Soc. LONDON Ser. A-MATHEMATICAL Phys. Eng. Sci.* **358**, 473 (2000).
- ² P.S. Weiser and S. Praver, *Diam. Relat. Mater.* **4**, 710 (1995).
- ³ J.G. Buijnsters, P. Shankar, W. Fleischer, W.J.P. van Enckevort, J.J. Schermer, and J.J. ter Meulen, *Diam. Relat. Mater.* **11**, 536 (2002).
- ⁴ F.J.G. Silva, A.J.S. Fernandes, F.M. Costa, A.P.M. Baptista, and E. Pereira, *Diam. Relat. Mater.* **13**, 828 (2004).
- ⁵ F.J.G. Silva, A.P.M. Baptista, and E. Pereira, *Diam. Relat. ...* **11**, 1617 (2002).
- ⁶ X. Xiao, B.W.W. Sheldon, E. Konca, L.C.C. Lev, and M.J.J. Lukitsch, *Diam. Relat. Mater.* **18**, 1114 (2009).
- ⁷ Q. Fan, A. Fernandes, and J. Gracio, *Diam. Relat. Mater.* **7**, 5 (1998).
- ⁸ J. Spinnewyn, M. Nesladek, and C. Asinari, *Diam. Relat. Mater.* **2**, 361 (1993).
- ⁹ a. Laikhtman, L. Rapoport, V. Perfiljev, A. Moshkovich, R. Akhvediani, A. Hoffman, S.C. Hendy, and I.W.M. Brown, *AIP Conf. Proc.* **157**, 157 (2009).
- ¹⁰ R. Haubner and B. Lux, *Int. J. Refract. Met. Hard Mater.* **24**, 380 (2006).
- ¹¹ S. Schwarz, S.M. Rosiwal, Y. Musayev, and R.F. Singer, *Diam. Relat. Mater.* **12**, 701 (2003).
- ¹² Y.-C. Chu, C.-H. Tu, G. Jiang, C. Chang, C. Liu, J.-M. Ting, H.-L. Lee, Y. Tzeng, and O. Auciello, *J. Appl. Phys.* **111**, 124328 (2012).
- ¹³ Y. Chu, G. Jiang, and C. Chang, ... (IEEE-NANO), 2011 ... 1367 (2011).
- ¹⁴ N.N. Naguib, J.W. Elam, J. Birrell, J. Wang, D.S. Grierson, B. Kabius, J.M. Hiller, A.V. Sumant, R.W. Carpick, O. Auciello, and J. a. Carlisle, *Chem. Phys. Lett.* **430**, 345 (2006).
- ¹⁵ C.Z. Zhang, H. Niakan, L. Yang, Y.S. Li, Y.F. Hu, and Q. Yang, *Surf. Coatings Technol.* **237**, 248 (2013).
- ¹⁶ G.A. Slack and S.F.F. Bartram, *J. Appl. Phys.* **46**, 89 (1975).
- ¹⁷ Böhler, 12 (2008).
- ¹⁸ *Binary Systems from Mn-Mo to Y-Zr*, edited by P. Franke and D. Neuschütz (Springer, Berlin Heidelberg, 2006), p. 313.
- ¹⁹ P.J. Kelly, *Vacuum* **56**, 159 (2000).
- ²⁰ E. Lassner and W.W.-D. Schubert, *Tungsten: Properties, Chemistry, Technology of the Elements, Alloys, and Chemical Compounds* (Springer Science & Business Media, New York, 1999), p. 422.
- ²¹ J. Gerth and U. Wiklund, *Wear* **264**, 885 (2008).
- ²² a. S. Kurlov and a. I. Gusev, *Inorg. Mater.* **42**, 121 (2006).
- ²³ H. Makita, K. Nishimura, N. Jiang, A. Hatta, T. Ito, and A. Hiraki, *Thin Solid Films* **281-282**, 279 (1996).
- ²⁴ M. Varga, T. Ižák, A. Kromka, M. Veselý, K. Hruška, and M. Michalka, *Cent. Eur. J. Phys.* **10**, 218 (2012).
- ²⁵ M. Varga, M. Vojs, M. Marton, L. Michalíková, M. Veselý, R. Redhammer, and M. Michalka, *Vacuum* **86**, 681 (2012).

- ²⁶ M. Daenen, O.A. Williams, J. D'Haen, K. Haenen, and M. Nesládek, *Phys. Status Solidi* **203**, 3005 (2006).
- ²⁷ S. Praver and R.J. Nemanich, *Philos. Trans. A. Math. Phys. Eng. Sci.* **362**, 2537 (2004).
- ²⁸ A.C. Ferrari and J. Robertson, *Phys. Rev. B* **63**, 121405 (2001).
- ²⁹ Y. Xie and H.M. Hawthorne, *Surf. Coatings Technol.* **155**, 121 (2002).
- ³⁰ P. Lu, H. Gomez, X. Xiao, M. Lukitsch, D. Durham, A. Sachdev, A. Kumar, and K. Chou, *Surf. Coatings Technol.* **215**, 272 (2013).
- ³¹ I. Endler, A. Leonhardt, H.-J. Scheibe, and R. Born, *Diam. Relat. Mater.* **5**, 299 (1996).
- ³² I.M. Hutchings, *Tribology: Friction and Wear of Engineering Materials* (Elsevier Ltd, 1992), p. 284.
- ³³ J.G. Buijnsters, P. Shankar, W.J.P.J.P. van Enckevort, J.J.J. Schermer, and J.J.J. ter Meulen, *Diam. Relat. Mater.* **13**, 848 (2004).
- ³⁴ J.J. Friel and C.E. Lyman, *Microsc. Microanal.* **12**, 2 (2006).